https://doi.org/10.1130/G51862.1

Manuscript received 4 November 2023 Revised manuscript received 3 March 2024 Manuscript accepted 15 March 2024

Published online 9 April 2024

© 2024 Geological Society of America. For permission to copy, contact editing@geosociety.org.

Bank strength variability and its impact on the system-scale morphodynamics of the upper Amazon River in Brazil

Muriel Z.M. Brückner^{1,*,†}, Rolf E. Aalto^{1,2}, Jim Best³, Renato Paes de Almeida⁴, Andrew P. Nicholas¹, Philip J. Ashworth⁵, and Marco lanniruberto⁶

- Department of Geography, Faculty of Environment, Science and Economy, University of Exeter, Exeter EX4 4SB, UK
- ²Department of Earth and Space Sciences, University of Washington, Seattle, Washington 98195, USA
- ³Departments of Earth Science and Environmental Change, Geography and Geographic Information Science, and Mechanical Science and Engineering, and Ven Te Chow Hydrosystems Laboratory, University of Illinois at Urbana-Champaign, Urbana, Illinois 61801, USA
- ⁴Department of Sedimentary and Environmental Geology, University of São Paulo, São Paulo 05508-220, Brazil
- ⁵School of Applied Sciences, University of Brighton, Brighton BN2 4AT, UK
- ⁶Department of Geosciences, University of Brasília, Brasília 70910-900, Brazil

ABSTRACT

Large anabranching rivers form channels in sediments of varying strength, resulting from erosional and depositional processes that act over geological time scales. Although bank strength variability is known to affect channel morphodynamics, its impact on the migration of large sand-bed rivers remains poorly understood. We report the first in situ measurements of bank strength from an $\sim\!100\text{-km}$ -long reach of the Solimões River, the Brazilian Amazon River upstream of Manaus. These show that cohesive muds in Pleistocene terraces along the river's right margin have bank strengths as much as three times greater than Holocene floodplain deposits composing the left bank. Image analysis suggests these resistant outcrops determine channel-bar dynamics: channel widening and bar deposition are inhibited, which lowers planform curvature and reduces erosion of the opposing bank. Planform analysis of the 1600-km-long Solimões River between 1984 and 2021 shows that where the channel is associated with Pleistocene terraces, lower rates of bank erosion and bar deposition are evident. Heterogeneity in bank strength is thus a first-order control on the large-scale morphodynamics of the world's largest lowland river.

INTRODUCTION

Large lowland sand-bed rivers develop anabranching channel patterns through the lateral migration of sinuous channels (Latrubesse, 2008). Migration is driven by morphodynamic feedbacks, whereby lateral erosion facilitates bar formation when channels widen (bank pull), which encourages steering of the flow toward the outer bank, promoting bank erosion (bar push) (Ashworth et al., 2000; Parker et al., 2011). These feedbacks depend on morphological and associated hydraulic characteristics (planform curvature, flow direction, bed topography) and

local bank strength, the latter controlling sediment resuspension and bank failure (Ashworth and Lewin, 2012; Zhao et al., 2022). River bank strength may be highly variable and is a function of local stratigraphy and sediment composition, grain size, diagenesis, and vegetation (Darby and Thorne, 1996; Motta et al., 2012). Although such variability controls local and reach-scale migration dynamics (Güneralp and Rhoads, 2011; Schwendel et al., 2015), studies have been limited to smaller single-threaded rivers, despite longstanding evidence that topographic and lithological variability are controls on many large rivers (Potter, 1978).

The Amazon River occupies a 100,000 km² wide Holocene floodplain incised into late Tertiary and Quaternary deposits (Mertes and Dunne, 2022). In central Amazonia, the interfluves between major rivers comprise fluvial deposits formed at a higher base level than

(Rossetti et al., 2015; Mertes and Dunne, 2022). Due to Holocene river incision, the active channel now frequently flows against, and along, these terraces. The Solimões River, the Brazilian Amazon River upstream of Manaus, has an anabranching channel belt that transitions from high sinuosity (1.6) to low sinuosity (1.1) near the confluence with the Japurá River (Mertes et al., 1996), accompanied by varying migration rates along both banks (Fig. 1A). This transition has been linked to changes in slope, underlying geology, and floodplain narrowing caused by older terraces (Mertes et al., 1996; Mertes and Dunne, 2022). However, these previous studies provided neither measurements nor detailed planform analyses. Herein, we hypothesize that PCCSs possess a higher bank strength than Holocene alluvium and that this difference controls large-scale river morphology and dynamics. We provide the first in situ measurements of bank strength along the Solimões River and compare these to reachscale morphodynamics from remotely sensed data. We quantify bank erosion and deposition rates along the entire Solimões River, demonstrate their dependence on the proximity

of the river to PCCSs, and provide a mecha-

nistic explanation for how variability in bank

the modern alluvial plain, originally mapped

as the Içá Formation (Maia et al., 1977) and

later revealed as Late Pleistocene in age (Ros-

setti et al., 2015; Pupim et al., 2019). Such

Pleistocene cohesive and cemented sediments

(PCCSs) form terraces tens of meters in eleva-

tion that comprise weakly consolidated fine-

to coarse-grained sand-, silt-, and mudstones

CITATION: Brückner, M.Z.M., et al., 2024, Bank strength variability and its impact on the system-scale morphodynamics of the upper Amazon River in Brazil: Geology, v. 52, p. 533–538, https://doi.org/10.1130/G51862.1

Muriel Z.M. Brückner **b** https://orcid.org/0000 .0002-7954-9586

^{*}mbruckner@lsu.edu

[†]Present address: Department of Civil and Environmental Engineering, Louisiana State University, Baton Rouge, Louisiana 70808, USA

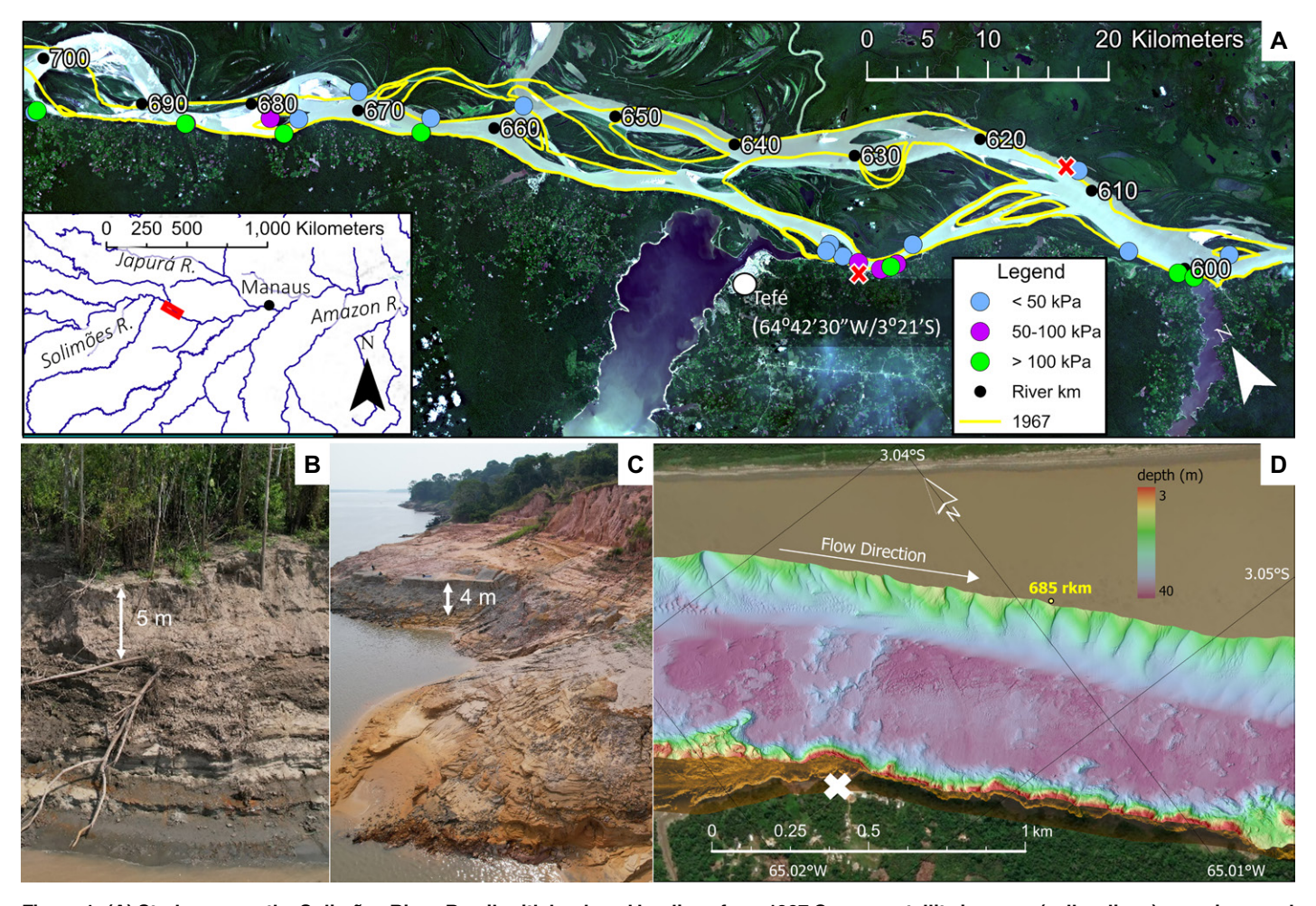


Figure 1. (A) Study area on the Solimões River, Brazil, with bank and bar lines from 1967 Corona satellite imagery (yellow lines) superimposed on 2021 PlanetScope imagery, showing varying migration rates between left and right bank. Colored points denote measurement locations along the 100 km reach of the Solimões River of three bank classes obtained with a shear vane. Inset map shows river network (HydroSHEDS database; Lehner and Grill, 2013) and study site location in the Amazon River basin (red rectangle). (B) Photograph of Holocene deposits on left bank, marked with red X. (C) Photograph of Pleistocene mud- and sandstones on right bank, marked with a red X. (D) Multibeam echo sounder and side-scan (<3 m; marked by X) data showing Pleistocene cohesive and cemented sediments (PCCSs; purple) outcrop along right bank and extending across channel, with margins of large sand dunes (green colors) in channel center. Depth is water depth based on the (low) stage during the field campaign. rkm—river kilometers.

strength exerts a first-order control on the migration behavior of one of the world's largest anabranching rivers.

METHODS

We briefly describe the methodology below, with more details provided in the Supplemental Material¹.

Field Data from the Solimões River

We collected 210 measurements of bank strength (Fig. 2) using a hand-held Pilcon shear vane and a cohesive strength meter (Mark III) at 30 locations along a 100 km reach of the Solimões River that has experienced contrasting

erosion between its south (right, looking downstream) and north (left, looking downstream) banks since 1967 (Fig. 1A). The shear vane (SV) records the axial strength of the top layer (He et al., 2018), whereas the cohesive strength meter (CSM) provides a critical shear stress for erosion based on a jet-pressure test (Tolhurst et al., 1999). To determine the morphology of submerged PCCSs, we collected multibeam echo sounder (MBES) and side-scan sonar data for the near-bank channel bed in October 2022 (low-flow stage). Side-scan return intensity data were overlain onto the processed MBES data, which were gridded at 0.25 m (see Supplemental Material).

Image and GIS Analyses

We digitized Corona satellite imagery from 11 December 1967 (U.S. Geological Survey, earthexplorer.usgs.gov; \sim 2 m resolution) and extracted bank and bar lines to compare

with Planet CubeSat data from October 2021 (\sim 3 m resolution; https://www.planet.com/). To quantify channel migration, we produced four-year composite images (1984-1988 and 2019-2023; Boothroyd et al., 2021) to classify water and land masks from Landsat imagery (see Supplemental Material) in three reaches along the Solimões River (Fig. 3A). These were classified as: (1) freely meandering (reach I), (2) partially constrained by PCCSs (reach II), and (3) partially constrained at the confluence with a secondary channel (reach III) based on digital elevation model data (FABDEM; https:// data.bris.ac.uk/data/dataset/25wfy0f9ukoge2gs7a5mqpq2j7) (Hawker et al., 2022; see Supplemental Material). In addition, we computed channel centerlines based on bank lines (RivMAP toolbox; Schwenk et al., 2017) to calculate channel sinuosity and mean annual erosion and deposition rates along each bank in 20 km or 10 km segments based on the river

¹Supplemental Material. Detailed description of the methodology. Please visit https://doi.org/10 .1130/GEOL.S.25439140 to access the supplemental material; contact editing@geosociety.org with any questions.

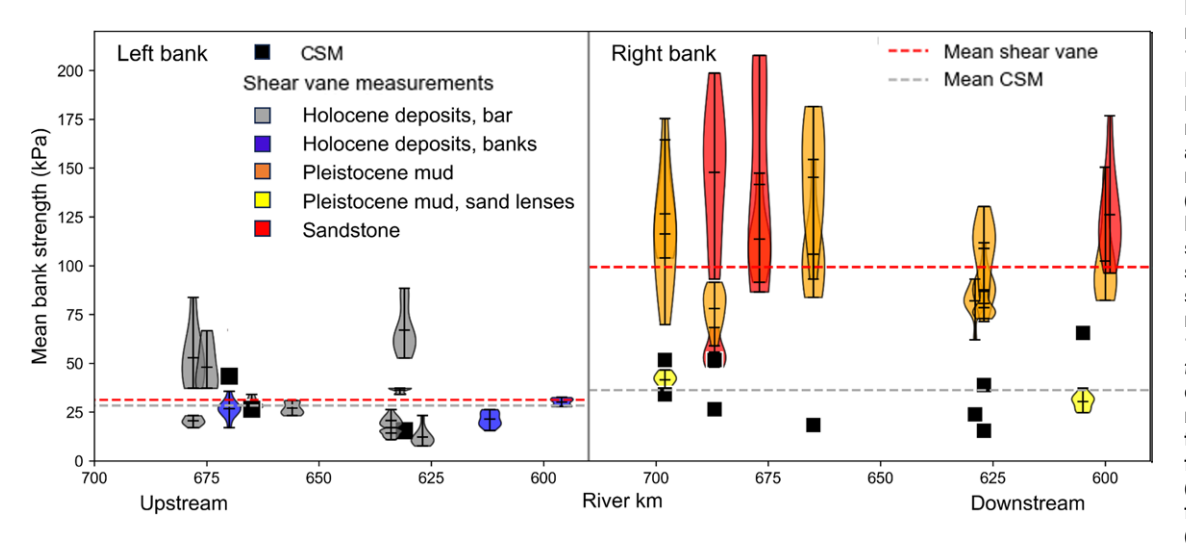


Figure 2. Bank strength measurements along 100 km reach of Solimões River (see Fig. 1A for location). Violin plots represent mean, and 25th and 75th percentiles, measured by shear vane (SV). Colors indicate lithological characteristics of samples; black squares show results from cohesive strength meter (CSM) multiplied by a factor of 10,000 to aid visibility. t-tests reveal significant differences between mean bank strengths on the left and right banks for SV measurements (p-value <0.05) but not for CSM (p-value >0.05) (see Supplemental Material [footnote 1]).

kilometers given in nautical charts (Brazilian Navy, 2001).

For the 1600 km of the Solimões River, the proximity of the bank line to PCCS terraces was measured at the scale of 10 km segments using FABDEM data (Hawker et al., 2022) by measuring the width of the adjacent Holocene floodplain (see Supplemental Material). Reaches were defined as "associated" with PCCSs when the distance from the nearest bank was less than the mean channel width. For banks in each reach, we measured changes in water and land areas from 1984 to 2021 using the Global Surface Water Explorer (https://global-surface-water .appspot.com; Pekel et al., 2016) to compute mean annual rates of erosion and deposition (see Supplemental Material).

RESULTS AND DISCUSSION Bank Sediments and Strength

We find notable differences in composition between the left-bank Holocene floodplain deposits and the right-bank PCCSs. Left banks and islands are characterized by sandy bar-top sediments (Fig. 1B) often overlain by mud drapes, whereas the right banks are a heterogeneous succession with frequent outcrops of elevated PCCSs (Fig. 1C). The fine-grained PCCS materials are commonly lithified by ferruginous cements, iron and manganese crusts, and ferruginous coatings along vertical fractures (Rossetti et al., 2015; Pupim et al., 2019). Cliff collapses, marked by slump blocks comprising claystones interpreted as Pleistocene lacustrine sediments, expose large clay outcrops (Fig. 1C).

These differences in deposits are reflected in our bank strength measurements: PCCS bank strength is variable but on average as much as three times greater than that of the Holocene deposits (SV in Fig. 2). PCCSs containing sandy lenses exhibit values closer to those of the left bank. The cohesive strength meter results reveal

no significant difference between the resistant PCCSs along the right bank and the Holocene deposits (Fig. 2; see the Supplemental Material). Differences between these two data sets reflect that the cohesive strength meter measures surface resuspension, related to hydraulic erosion processes, while the shear vane measures strength within a deeper surface layer, linked to mechanical bank failure (Tolhurst et al., 1999; He et al., 2018).

MBES and side-scan sonar images illustrate the prevalence of PCCSs from bank top to toe (see also the Supplemental Material), commonly extending far into the main channel (Fig. 1D). These outcrops influence channel migration rates by locally reducing vertical and lateral erodibility, altering the flow dynamics, controlling the steering of bedload sediment, and providing local bank and bed protection. Such mechanisms have been highlighted in previous studies that have detailed the role of both nearbank bedrock (Nittrouer et al., 2011; Konsoer et al., 2016) and slump blocks associated with intermittent bank failures (Hackney et al., 2015). However, in those cases, bedrock outcrops were located either at the outer bank of sinuous channels or where channel curvature promoted deep scouring. PCCS outcrops documented herein are common along large stretches of the right bank of the Solimões River and the adjacent bed where channel curvature is low.

Reach- and System-Scale Dynamics

To assess the role of bank strength variability on erosion and deposition, we investigated three reaches classified as freely meandering or partially constrained (Fig. 3A). Figures 3B and 3C show an increasing asymmetry between erosion and deposition from reach I to reach III where PCCSs were present (with the exception of segment B2). Bank erosion and deposition are balanced throughout reach I, where PCCSs are

absent and sinuosity is highest (1.33). Diminishing erosion along the right bank is linked to the presence of resistant layers in reach II (gray shades in Fig. 3C), where net bar deposition also decreases, indicating reduced bar formation and lower sinuosity (1.24). The main channel of reach III becomes stable when encountering the PCCSs, which promotes reduced left-bank erosion through low deposition and channel sinuosity (1.15). The secondary channel, which flows entirely along the resistant layers (see Fig. 3A), remains stable along both banks with low erosion and deposition.

These trends illustrate that channel sinuosity and migration are strongly controlled by bank strength variability as recorded with the shear vane (Fig. 3): high bank strength along one bank inhibits lateral erosion, which reduces local and downstream sediment availability, point bar deposition, and steering of the flow. In the Amazon River, a substantial proportion of locally transported sediment originates from the floodplain, sourced through bank erosion and collapse (Dunne et al., 1998), which drives meandering through positive feedbacks between sediment flux and bar formation (Constantine et al., 2014). Such feedbacks are interrupted by the presence of PCCSs, which resist erosion and affect supply of bedload-sized material, evidenced by the absence of dunes near the PCCS banks (Fig. 1D). The lack of bedforms implies that transport capacities exceed sediment supply for hundreds of meters from the bank, thus inhibiting bar deposition and maintaining channel position adjacent to the PCCS outcrops. The absence of flow steering due to lower channel curvature also stabilizes the left bank, despite the latter comprising more erodible alluvium. Resistance of the top sediment layer to failure (representative of the shear vane results) is likely to be the main control here compared to surface erosion processes. Although demanding future

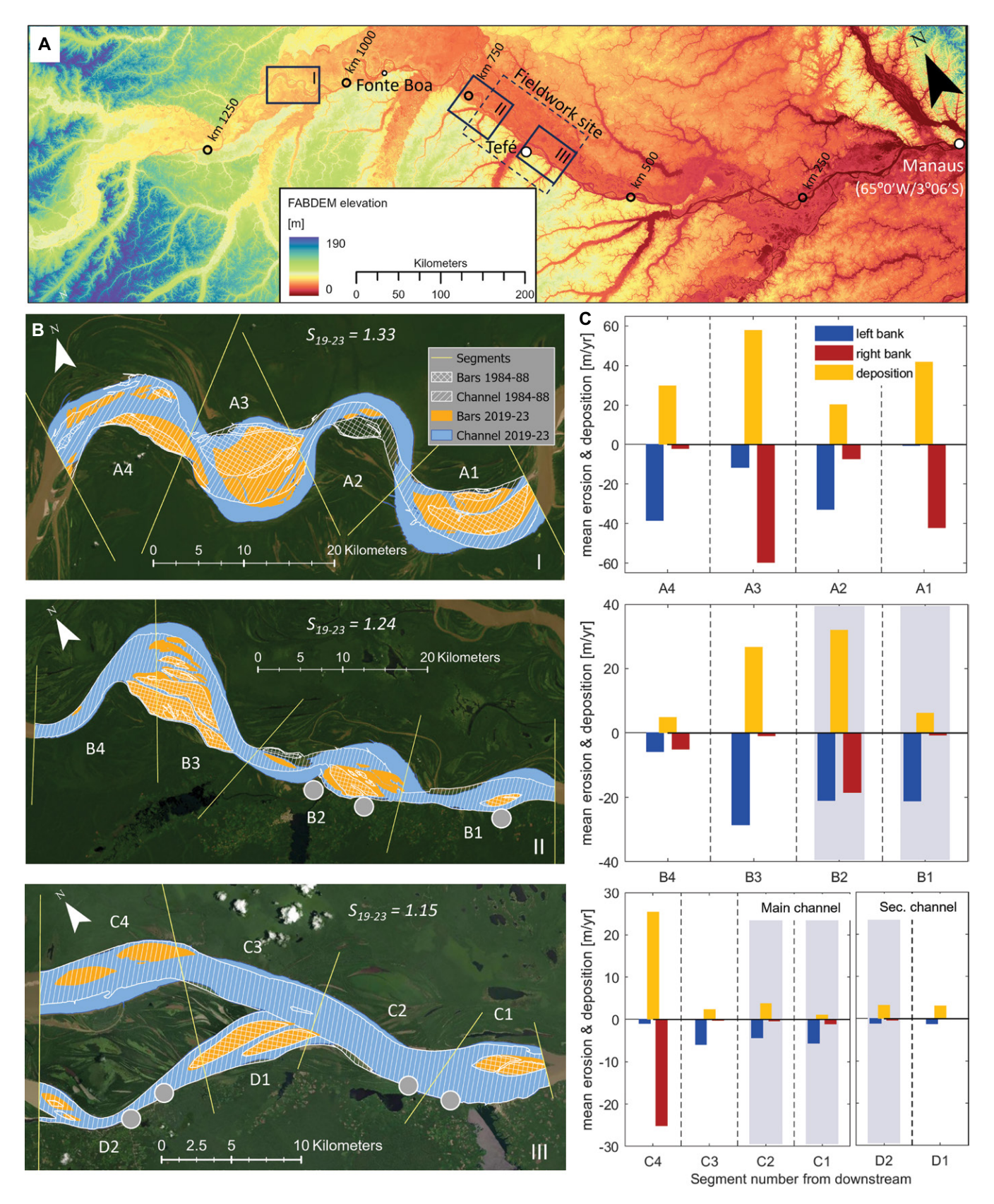


Figure 3. (A) Digital elevation model (FABDEM) of the Solimões River with locations of a freely meandering reach (I) (river km 1040–1120), a partially constrained reach at the confluence with a secondary channel (III) (river km 590–630). Fieldwork site is indicated (dashed rectangle). (B) Overlays of channel and bar area averaged between 1984–1988 (white hatched areas) and 2019–2023 (blue and orange areas) derived from Landsat imagery. Yellow lines indicate segments of \sim 20 km (reaches I and II) and 10 km (reach III) width; gray circles denote locations of measured resistant layers. S_{19-23} —mean sinuosity for years 2019–2023. (C) Bank erosion (negative values) along each bank and net deposition (positive values) averaged over each segment compared to locations of resistant layers (shear vane measurements >100 kPa) observed in the field marked as gray shades. Sec.—secondary.

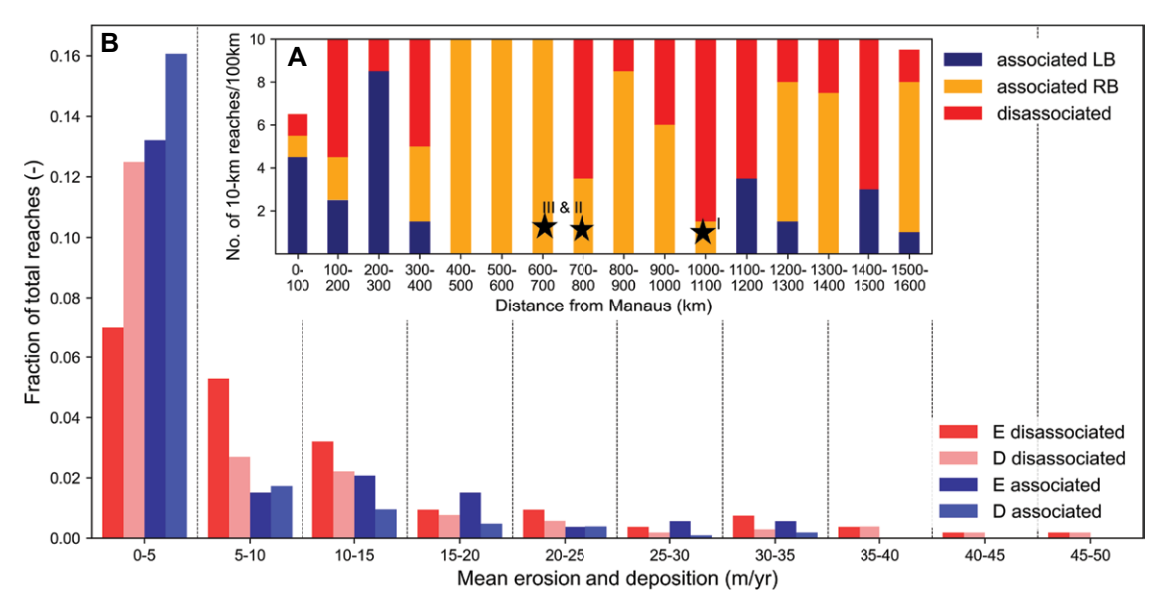


Figure 4. (A) Number of reaches classified as associated and disassociated with PCCSs with distance from Manaus (LB-left bank; RB-right bank). Reaches in present study are marked as stars for context. (B) Fraction of associated and disassociated reaches versus mean erosion (E) and deposition (D) rate. Two-sample Kolmogorov-Smirnoff tests for erosion and deposition show significantly different distributions between the associated and disassociated reaches for erosion and deposition (p-values < 0.05) (see Supplemental Material [see text footnote 1]).

measurements of flow to test such reasoning, our observations provide a mechanistic link between the presence of PCCSs and channel migration. Previous studies have suggested that changes in sinuosity and channel migration rates along the Solimões River are related to changes in slope and underlying geology (Dunne et al., 1998; Birkett et al., 2002; Dunne and Aalto, 2013). Our data show that bank strength is a primary control on differences in channel pattern in the Solimões River, with the stable right bank suppressing bank erosion and limiting creation of sinuous channels (Kleinhans et al., 2024), which thereby stabilizes both banks of the active channel.

Our GIS analysis over 1600 km shows that the main channel frequently flows close to the higher terraces (Fig. 4A; Supplemental Material), which are likely similar to the PCCSs documented herein (Rossetti et al., 2015; Pupim et al., 2019). Reaches with the highest rates of erosion and deposition are disassociated from PCCSs, whereas reaches associated with PCCSs exhibit reduced erosion and deposition rates. PCCSs therefore may influence larger-scale dynamics in the Solimões River through the morphodynamic mechanisms proposed above, with possible implications for the controls on other large sand-bed rivers where PCCS deposits have been reported, such as the Orinoco River (Venezuela and Colombia; Warne et al., 2002), Late Holocene Willamette River (Oregon, USA; Wallick et al., 2022), Mekong River (East and Southeast Asia: Carling, 2009), and lower Mississippi River (central United States; Nittrouer et al., 2011).

CONCLUSIONS

A 100-km-long reach of the Solimões River studied herein is characterized by Holocene floodplain deposits along its left bank and Pleistocene cohesive and cemented sediments (PCCSs) along its right bank. Shear vane measurements show bank strength to be as much

as three times greater along the right bank as compared to the left bank. In reaches where PCCSs are present, erosion and deposition rates are reduced, influencing channel sinuosity and migration. We argue that bar formation is suppressed along the right bank due to limited channel widening and associated low sediment supply from the resistant PCCSs. This reduced bar formation impedes steering of the flow and development of channel curvature, thereby lessening erosion of the weaker left bank in the downstream direction. Migration analysis for the 1600-km-long river reveals that erosion and deposition decrease in reaches associated with PCCSs, suggesting that these feedbacks affect sinuosity and lateral dynamics in the Solimões River and potentially other large lowland rivers that possess significant PCCSs.

ACKNOWLEDGMENTS

This project was funded by the UK Natural Environment Research Council (NERC) grant NE/T007478/1. We thank Liliane Janikian Paes de Almeida, Felipe Figueiredo, Pedro Gomes, and Carlos Manjon Mazoca for field support, the U.S. Geological Survey for the Corona imagery, RuralTech for the MBES survey, Planet Labs Inc. for satellite imagery, and Steve Darby for the cohesive strength meter. Comments from Thomas Dunne and two anonymous reviewers significantly improved the manuscript. For the purpose of open access, the author has applied a Creative Commons Attribution (CC BY) license to any author accepted manuscript version arising from this submission. The research data, measurements, GIS data, and Landsat, CORONA, and MBES imagery, are openly available at https://doi.org/10.5285/11786f86-a3ac-45ab-81b5-10fd157e3d7a.

REFERENCES CITED

Ashworth, P.J., and Lewin, J., 2012, How do big rivers come to be different?: Earth-Science Reviews, v. 114, p. 84–107, https://doi.org/10.1016/j.earscirev.2012.05.003.

Ashworth, P.J., Best, J.L., Roden, J.E., Bristow, C.S., and Klaassen, G.J., 2000, Morphological evolution and dynamics of a large, sand braid-bar,

Jamuna River, Bangladesh: Sedimentology, v. 47, p. 533–555, https://doi.org/10.1046/j.1365-3091.2000.00305.x.

Birkett, C.M., Mertes, L.A.K., Dunne, T., Costa, M.H., and Jasinski, M.J., 2002, Surface water dynamics in the Amazon Basin: Application of satellite radar altimetry: Journal of Geophysical Research, v. 107, 8059, https://doi.org/10.1029/2001JD000609.

Boothroyd, R.J., Williams, R.D., Hoey, T.B., Barrett, B., and Prasojo, O.A., 2021, Applications of Google Earth Engine in fluvial geomorphology for detecting river channel change: Wiley Interdisciplinary Reviews: Water (Basel), v. 8, https://doi.org/10.1002/wat2.1496.

Brazilian Navy, 2001, Nautical charts: Directory of Hydrography and Navigation of Brazilian Navy, https://www.marinha.mil.br/emgepron/en-us/nautical-charts.

Carling, P.A., 2009, Geomorphology and sedimentology of the Lower Mekong River, *in* Campbell, I.C., ed., The Mekong: Biophysical Environment of an International River Basin: New York, Elsevier, p. 77–111, https://doi.org/10.1016/B978-0-12-374026-7.00005-X.

Constantine, J.A., Dunne, T., Ahmed, J., Legleiter, C., and Lazarus, E.D., 2014, Sediment supply as a driver of river meandering and floodplain evolution in the Amazon Basin: Nature Geoscience, v. 7, p. 899–903, https://doi.org/10.1038/ngeo2282.

Darby, S.E., and Thorne, C.R., 1996, Development and testing of riverbank-stability analysis: Journal of Hydraulic Engineering, v. 122, p. 443–454, https://doi.org/10.1061/(ASCE)0733-9429(1996)122:8(443).

Dunne, T., and Aalto, R.E., 2013, Large river flood-plains, *in* Wohl, E., ed., Treatise on Geomorphology, Volume 9: Fluvial Geomorphology: London, Elsevier, v. 9, p. 645–678, https://doi.org/10.1016/B978-0-12-374739-6.00258-X.

Dunne, T., Mertes, L.A.K., Meade, R.H., Richey, J.E., and Forsberg, B.R., 1998, Exchanges of sediment between the flood plain and channel of the Amazon River in Brazil: Geological Society of America Bulletin, v. 110, p. 450–467, https://doi.org/10.1130/0016-7606(1998)110<0450: EOSBTF>2.3.CO:2.

Güneralp, İ., and Rhoads, B.L., 2011, Influence of floodplain erosional heterogeneity on planform complexity of meandering rivers: Geophysical Research Letters, v. 38, L14401, https://doi.org /10.1029/2011GL048134.

- Hackney, C., Best, J., Leyland, J., Darby, S.E., Parsons, D., Aalto, R., and Nicholas, A., 2015, Modulation of outer bank erosion by slump blocks: Disentangling the protective and destructive role of failed material on the three-dimensional flow structure: Geophysical Research Letters, v. 42, p. 10,663–10,670, https://doi.org/10.1002/2015GL066481.
- Hawker, L., Uhe, P., Paulo, L., Sosa, J., Savage, J., Sampson, C., and Neal, J., 2022, A 30 m global map of elevation with forests and buildings removed: Environmental Research Letters, v. 17, 024016, https://doi.org/10.1088/1748-9326/ac4d4f.
- He, C., You, Y., Wang, D., and Wu, H., 2018, Estimating soil failure due to torsion via vane shear test by varying vane diameter and soil properties: Soil and Tillage Research, v. 177, p. 68–78, https://doi.org/10.1016/j.still.2017.12.004.
- Kleinhans, M.G., McMahon, W.J., and Davies, N.S., 2024, What even is a meandering river? A philosophy-enhanced synthesis of multi-level causes and systemic interactions contributing to river meandering, in Finotello, A., et al., eds., Meandering Streamflows: Patterns and Processes across Landscapes and Scales: Geological Society, London, Special Publication 540, https://doi.org/10.1144/SP540-2022-138.
- Konsoer, K.M., Rhoads, B.L., Langendoen, E.J., Best, J.L., Ursic, M.E., Abad, J.D., and Garcia, M.H., 2016, Spatial variability in bank resistance to erosion on a large meandering, mixed bedrockalluvial river: Geomorphology, v. 252, p. 80–97, https://doi.org/10.1016/j.geomorph.2015.08.002.
- Latrubesse, E.M., 2008, Patterns of anabranching channels: The ultimate end-member adjustment of mega rivers: Geomorphology, v. 101, p. 130–145, https://doi.org/10.1016/j.geomorph 2008 05 035
- Lehner, B., and Grill, G., 2013, Global river hydrography and network routing: Baseline data and new approaches to study the world's large river systems: Hydrological Processes, v. 27, p. 2171–2186, https://doi.org/10.1002/hyp.9740.
- Maia, R.G.N., Godoy, H.K., Yamaguti, H.S., de Moura, P.A., Ferreira da Costa, F.S., Arcanjo de Holanda, M., and Alencar de Costa, J., 1977, Projeto carvão no Alto Solimões: Relatório final: Manaus, Serviço Geológico do Brasil (CPRM)—

- Departamento Nacional de Produção Mineral (DNPM), 267 p.
- Mertes, L.A.K., and Dunne, T., 2022, Effects of tectonism and sea-level change on the form and behaviour of the modern Amazon River and its floodplain, *in* Gupta, A., ed., Large Rivers: Geomorphology and Management (2nd edition): Hoboken, New Jersey, John Wiley & Sons, p. 171–204, https://doi.org/10.1002/9781119412632.ch8.
- Mertes, L.A.K., Dunne, T., and Martinelli, L.A., 1996, Channel-floodplain geomorphology along the Solimões-Amazon River: Geological Society of America Bulletin, v. 108, p. 1089–1107, https:// doi.org/10.1130/0016-7606(1996)108<1089: CFGATS>2.3.CO;2.
- Motta, D., Abad, J.D., Langendoen, E.J., and García, M.H., 2012, The effects of floodplain soil heterogeneity on meander planform shape: Water Resources Research, v. 48, W09518, https://doi .org/10.1029/2011WR011601.
- Nittrouer, J.A., Mohrig, D., Allison, M.A., and Peyret, A.P.B., 2011, The lowermost Mississippi River: A mixed bedrock-alluvial channel: Sedimentology, v. 58, p. 1914–1934, https://doi.org/10.1111/j.1365-3091.2011.01245.x.
- Parker, G., Shimizu, Y., Wilkerson, G.V., Eke, E.C., Abad, J.D., Lauer, J.W., Paola, C., Dietrich, W.E., and Voller, V.R., 2011, A new framework for modeling the migration of meandering rivers: Earth Surface Processes and Landforms, v. 36, p. 70–86, https://doi.org/10.1002/esp .2113.
- Pekel, J.F., Cottam, A., Gorelick, N., and Belward, A.S., 2016, High-resolution mapping of global surface water and its long-term changes: Nature, v. 540, p. 418–422, https://doi.org/10.1038/ nature/20584
- Potter, E.P., 1978, Significance and origin of big rivers: Journal of Geology, v. 86, p. 13–33, https://doi.org/10.1086/649653.
- Pupim, F.N., et al., 2019, Chronology of Terra Firme formation in Amazonian lowlands reveals a dynamic Quaternary landscape: Quaternary Science Reviews, v. 210, p. 154–163, https://doi.org/10.1016/j.quascirev.2019.03.008.
- Rossetti, D.F., et al., 2015, Mid-Late Pleistocene OSL chronology in western Amazonia and implica-

- tions for the transcontinental Amazon pathway: Sedimentary Geology, v. 330, p. 1–15, https://doi.org/10.1016/j.sedgeo.2015.10.001.
- Schwendel, A.C., Nicholas, A.P., Aalto, R.E., Sambrook Smith, G.H., and Buckley, S., 2015, Interaction between meander dynamics and floodplain heterogeneity in a large tropical sand-bed river: The Rio Beni, Bolivian Amazon: Earth Surface Processes and Landforms, v. 40, p. 2026–2040, https://doi.org/10.1002/esp.3777.
- Schwenk, J., Khandelwal, A., Fratkin, M., Kumar, V., and Foufoula-Georgiou, E., 2017, High spatiotemporal resolution of river planform dynamics from Landsat: The RivMAP toolbox and results from the Ucayali River: Earth and Space Science (Hoboken, New Jersey), v. 4, p. 46–75, https://doi.org/10.1002/2016EA000196.
- Tolhurst, T.J., Black, K.S., Shayler, S.A., Mather, S., Black, I., Baker, K., and Paterson, D.M., 1999, Measuring the in situ erosion shear stress of intertidal sediments with the Cohesive Strength Meter (CSM): Estuarine, Coastal and Shelf Science, v. 49, p. 281–294, https://doi.org/10.1006/ecss.1999.0512.
- Wallick, J.R., Grant, G., Lancaster, S., Bolte, J.P., and Denlinger, R., 2022, Patterns and controls on historical channel change in the Willamette River, Oregon, USA, *in* Gupta, A., ed., Large Rivers: Geomorphology and Management (2nd edition): Hoboken, New Jersey, John Wiley & Sons, p. 737–775, https://doi.org/10.1002/9781119412632.ch25.
- Warne, A.G., Meade, R.H., White, W.A., Guevara, E.H., Gibeaut, J., Smyth, R.C., Aslan, A., and Tremblay, T., 2002, Regional controls on geomorphology, hydrology, and ecosystem integrity in the Orinoco Delta, Venezuela: Geomorphology, v. 44, no. 3–4, p. 273–307, https://doi.org/10.1016/S0169-555X(01)00179-9.
- Zhao, K., Coco, G., Gong, Z., Darby, S.E., Lanzoni, S., Xu, F., Zhang, K., and Townend, I., 2022, A review on bank retreat: Mechanisms, observations, and modeling: Reviews of Geophysics, v. 60, https://doi.org/10.1029/2021RG000761.

Printed in the USA